DOI:
10.1016/j.bbamem.2017.07.015

Document Version
Peer reviewed version

Functional Mapping of the N-terminal Arginine Cluster and C-terminal Acidic Residues of Kir6.2 channel Fused to a G Protein-Coupled Receptor

Maria A. Principalli, Laura Lemel, Anaëlle Rongier, Anne-Claire Godet, Karla Langer, Jean Revilloud, Leonardo Darré, Carmen Domene, Michel Vivaudou, Christophe J. Moreau

PII: S0005-2736(17)30240-7
DOI: doi:10.1016/j.bbamem.2017.07.015
Reference: BBAMEM 82548

To appear in: *BBA - Biomembranes*

Received date: 3 April 2017
Revised date: 6 July 2017
Accepted date: 26 July 2017

Please cite this article as: Maria A. Principalli, Laura Lemel, Anaëlle Rongier, Anne-Claire Godet, Karla Langer, Jean Revilloud, Leonardo Darré, Carmen Domene, Michel Vivaudou, Christophe J. Moreau, Functional Mapping of the N-terminal Arginine Cluster and C-terminal Acidic Residues of Kir6.2 channel Fused to a G Protein-Coupled Receptor, *BBA - Biomembranes* (2017), doi:10.1016/j.bbamem.2017.07.015

Functional Mapping of the N-terminal Arginine Cluster and C-terminal Acidic Residues of Kir6.2 channel Fused to a G Protein-Coupled Receptor

Maria A. Principalli[a], Laura Lemel[a], Anaëlle Rongier[a, 1], Anne-Claire Godet[a, 2], Karla Langer[a], Jean Revilloud[a], Leonardo Darré[b, 3], Carmen Domene[b, c], Michel Vivaudou[a] and Christophe J. Moreau[a].

[a] Institut de Biologie Structurale (IBS), Univ. Grenoble Alpes, CEA, CNRS, LabEx ICST, 71, avenue des Martyrs, CS10090, F-38044 Grenoble, France
[b] Department of Chemistry, King's College London, Britannia House, 7 Trinity Street, London SE1 1DB, UK
[c] Chemistry Research Laboratory, University of Oxford, 12 Mansfield Road, Oxford OX1 3TA, UK.

***Correspondence to Christophe J. Moreau**. Institut de Biologie Structurale, Channels Group, 71, avenue des Martyrs, CS10090, F-38044 Grenoble, France. Telephone: (33) 457 428 579, Fax: (33) 476 501 890. christophe.moreau@ibs.fr*

[1] Present address: UMR5249-Laboratoire de Chimie et Biologie des Métaux (CEA/CNRS/UGA), BIG, CEA-Grenoble, 17 rue des Martyrs, F-38000 Grenoble, France & UMR5819-Laboratoire Structures et Propriétés d'Architectures Moléculaires (CEA/CNRS/UGA), INAC, CEA-Grenoble, 17 rue des Martyrs, F-38000 Grenoble, France

[2] Present address: Inserm U1048, I2MC (Institut des Maladies Métaboliques et Cardiovasculaires), F-31432, Toulouse, France

[3] Present address: Institute for Research in Biomedicine (IRB Barcelona). The Barcelona Institute of Science and Technology & Joint BSC-IRB Program in Computational Biology, 08028 Barcelona, Spain

Abbreviations

ACh, acetylcholine; atm, atmosphere; C-ter, C-terminus; D2, $D2_L$ dopaminergic receptor; GPCR, G protein-coupled receptor; ICCR: Ion Channel-Coupled Receptor; N-ter: N-terminus; TEVC, two-electrode voltage-clamp.

AbstractIon channel-coupled receptors (ICCRs) are original man-made ligand-gated ion channels created by fusion of G protein-coupled receptors (GPCRs) to the inward-rectifier potassium channel Kir6.2. GPCR conformational changes induced by ligand binding are transduced into electrical current by the ion channel. This functional coupling is closely related to the length of the linker region formed by the GPCR C-terminus (C-ter) and Kir6.2 N-terminus (N-ter). Manipulating the GPCR C-ter length allows to finely tune the channel regulation, both in amplitude and sign (opening or closing Kir6.2). In this work, we demonstrate that the primary sequence of the channel N-terminal domain is an additional parameter for the functional coupling with GPCRs. As for all Kir channels, a cluster of basic residues is present in the N-terminal domain of Kir6.2 and is composed of 5 arginines which are proximal to the GPCR C-ter in the fusion proteins. Using a functional mapping approach, we demonstrate the role of specific arginines (R27 and R32) for the function of ICCRs, indicating that the position and not the cluster of positively-charged arginines is critical for the channel regulation by the GPCR. Following observations provided by molecular dynamics simulation, we explore the hypothesis of interaction of these arginines with acidic residues, and using site-directed mutagenesis, we identified aspartate D307 and glutamate E308 residues as critical for the function of ICCRs. These results demonstrate the critical role of the N-terminal and C-terminal charged residues of Kir6.2 for its allosteric regulation by the fused GPCR.

Keywords

ion channel-coupled receptor (ICCR); protein engineering; electrophysiology; muscarinic receptor, molecular dynamics simulations.

1. Introduction

Ligand-gated ion channels are ionotropic receptors that transduce binding of biochemical messengers, such as neurotransmitters, into electrical current. We created artificial ligand-gated ion channels by fusing the C-ter of G protein-coupled receptors (GPCRs) to the N-ter of the potassium Kir6.2 channel [1]. In order to create a functional coupling between the two proteins, the length of the linking region had to be adjusted by deletion of the channel N-ter with an optimum deletion of 25 residues. These fusion proteins called Ion Channel-Coupled Receptors (ICCRs) act as the natural ligand-gated ion channels by generating an electrical signal upon binding of extracellular ligands to the receptor. Thus, Kir6.2 channel gating is regulated by the conformational changes of the fused GPCR. While natural ligand-gated ion channels recognize a limited number of endogenous ligands, ICCRs allow to expand the repertoire of recognized molecules to that of the natural GPCR ligands. Moreover, ICCRs have the advantage of being potassium-selective and to generate sustained signals over several minutes while natural ligand-gated cationic channels are poorly selective and desensitize within seconds [2]. Unexpectedly, in the first designed ICCRs, the regulation of Kir6.2 occurred in two opposite ways depending on the fused GPCR; the human M2 muscarinic receptor opened the channel upon agonist binding while the human $D2_L$ (D2) dopaminergic receptor closed it. Noting that the C-ter of the M2 receptor is 9 residues longer than the C-ter of $D2_L$, the length of both C-termini was inverted (shortening M2 and extending D2 with different sequences). The result was an inversion of the channel regulation indicating that the C-ter of these GPCRs is involved in the activating and inhibitory regulation of the channel. Subsequently, we demonstrated that the length of the GPCR C-ter controls the sign of the signal independently of its primary sequence. Notably, the ability to finely tune the Kir6.2 channel regulation by engineering the C-ter of fused GPCRs opens perspectives in synthetic biology to control cellular responses to endogenous or exogenous ligands [3]. However, the molecular mechanisms of this allosteric regulation have not yet been characterized, and some GPCR are difficult to functionally couple to the ion channel. While the current semi-empiric approach was based on alignments of GPCR C-termini

to adjust their length to the one of M2 and D2, the objective of this structure-function study is to identify residues in the Kir6.2 domains critical for the regulation of the ion channel. A better knowledge of the domains involved in the propagation of conformational changes between the receptor and the channel will help to push forward the rational design of ICCRs.
In this work, we found that, while deletion of 9 residues of the M2 C-ter inverted the channel regulation, the same length of deletion in the channel N-ter abolished it. The difference of phenotype is only explained by the difference in the amino acid composition of the 9 residues as both constructs are isometric. Using a rational functional mapping approach, we identify residues in the Kir6.2 N-terminal (R27, R32) and C-terminal (D307, E308) domains that are implicated in ICCR regulation.

2. Materials and Methods

Materials

Acetylcholine chloride was purchased from Sigma-Aldrich. The stock solution was 5 mM in ultrapure water.

2.1. Genetic engineering

All genes were in pGEMHE-derived vectors, optimized for protein expression in *Xenopus* oocytes. The templates M2=K0-25 and M2=K-9-25 were created in an earlier study by two-step PCR [1,4]. Truncations of the Kir6.2 N-ter were performed by one-step PCR with the QuikChange site-directed mutagenesis kit (Agilent) using primers overlapping deleted sequences. Site-directed mutations were performed using the same kit with primers containing mutations. Positive clones were verified by sequencing. DNA was amplified using Qiagen MidiPrep Kit, then linearized in the 3' region of the polyA tail and finally purified by standard phenol:chloroform extraction before its transcription in mRNA using the T7 mMessage mMachine Kit (Thermo Fisher Scientific). mRNAs were purified with the standard phenol:chloroform protocol, analyzed by agarose-gel electrophoresis and quantified by spectrophotometry [5,6].

Electrophysiological recordings

Xenopus oocytes were prepared as previously reported [1,4]. Animal handling and experiments fully conformed with European regulations and were approved by the Ethics Committee of the Commissariat à l'Energie Atomique et aux Energies Alternatives (Ethics Approval #12-040 to Christophe Moreau). Authorization of the animal facility has been delivered by the Prefect of Isere (Authorization # D 38 185 10 001).

Briefly, after surgical retrieval, the oocytes were defolliculated by type 1A collagenase. Each oocyte was injected with 50 nl of RNAse-free water containing the desired mRNAs. The amount used per oocyte was 4.3 ng. Microinjected oocytes were incubated for more than 2 days at 19°C in Barth's solution (in mM: 1 KCl, 0.82 $MgSO_4$, 88 NaCl, 2.4 $NaHCO_3$, 0.41 $CaCl_2$, 16 Hepes, pH 7.4) supplemented with 100 $U.ml^{-1}$ of penicillin and streptomycin and 0.1 $mg.ml^{-1}$ of gentamycin. Whole-cell currents were recorded with the two-electrode voltage-clamp (TEVC) technique either manually or automated with the HiClamp robot (MultiChannel Systems). Microelectrodes were filled with 3 M KCl, and oocytes were bathed during recordings in the following solution (TEVC bath, in mM): 91 KCl, 1.8 $CaCl_2$, 1 $MgCl_2$, 5 HEPES, 0.3 niflumic acid (to block endogenous Cl^- currents), pH 7.4. The manual TEVC voltage protocol consisted of 500 ms steps to -50, 0 and +50 mV, during which current was measured, separated by 5 s at a holding potential of 0 mV. The values shown in the Figures are those recorded at -50 mV. During recordings with the HiClamp robot, the membrane potential was clamped to -50 mV.

Average values are presented as mean±s.e.m. The number of recordings (n) is shown besides the bars and represents the number of tested oocytes. Ba^{2+} (3 mM) was used as a generic potassium channel blocker to establish the amplitude of potassium currents. Change of

potassium current induced by ligand was calculated with the barium-sensitive current as reference.

2.2. Molecular Dynamics (MD) Simulations

Until very recently, no experimental structures for the wild-type Kir6.2 channel were available, compelling the use of homology modelling in order to obtain initial coordinates suitable for molecular dynamics simulations, as was the case in the present contribution. For this purpose, the crystal structure of Kir2.2 (PDB ID: 3SPI), resolved at a resolution of 3.3 Å, and showing a 50.3% sequence identity with Kir6.2, was used as structural template. The sequence of the human Kir6.2 channel (Uniprot ID: Q14654) and the Kir2.2 X-ray template were fed to MODELLER9.11; the best predicted model was selected as the input of subsequent MD simulations. The metric used to define such best model was the statistical potential called DOPE (Discrete Optimized Protein Energy) [7], which excels in identifying native-like structures (lowest DOPE values). Extra residues in the N-ter segment (A22 to Q30) were added in random conformation, allowing for the unbiased structural exploration of an N-ter domain containing the cluster of positive residues of interest. PIO ([(2R)-2-octanoyloxy-3-[oxidanyl-[(1R,2R,3S,4R,5R,6S)-2,3,6-tris(oxidanyl)-4,5-diphosphonooxy-cyclohexyl]oxy- phosphoryl]oxy-propyl] octanoate) molecules present in the Kir2.2 crystal structure were kept, and used to reconstruct PIP_2 molecules. An initial water shell was added to the Kir6.2-PIP_2 complex using the SOLVATE software, which facilitates the hydration of the central pore of the channel. The obtained partially solvated channel-PIP_2 complex was embedded in a pre-equilibrated lipid bilayer of 1-palmitoyl-2-oleoyl-sn-glycero-3-phosphocholine (POPC) molecules, with the channel axis aligned to the bilayer normal, and the hydrophobic transmembrane domain (TMD) aligned with the bilayer. Lipid molecules overlapping with protein atoms, as well as water molecules overlapping with lipid atoms, were removed. This procedure resulted in a lipid bilayer consisting of 700 POPC molecules. The system was further solvated using the *Solvate* plug-in of VMD and water molecules within 1.2 Å of previously added water, protein or lipid atoms were removed. Ions were added to the system to achieve neutralization, up to a final concentration of 150 mM KCl. Two potassium ions in the selectivity filter of the crystal structure were kept while the two other were modeled as water molecules. The CHARMM22/CMAP force field was used to represent the protein, CHARMM36 [8] was used for the lipids, the TIP3P model [9] for water, and the standard CHARMM and NBFIX parameters were used for ions [10,11]. Parameters for PIP_2 molecules were as proposed in [12]. The energy of the system was minimized in 5,000 steps of geometry optimization, and equilibration at 310 K and 1 atm was achieved following a sequence of short MD simulations in the NpT ensemble: (i) 500 ps with restraints on the protein, the water in the cavity, and the crystallographic potassium ions. Correct lipid packing against the TMD was achieved using the NAMD Tcl Forces module that excludes water molecules diffusing into the TMD-bilayer interface; (ii) 500 ps with restraints on the protein backbone atoms; (iii) 500 ps applying restraints on the selectivity filter. Semi-isotropic pressure coupling at 1 atm was accomplished using the Nose-Hoover Langevin piston [13] while temperature was maintained at 310 K by means of the Langevin thermostat [14]. The particle mesh Ewald algorithm [15] (grid spacing of 1Å) was used for long-range electrostatic interactions and van der Waals forces were smoothly switched off between 10-12 Å. A Verlet neighbor list with pairlist distance of 13 Å was used. Equations of motions were integrated using the multi time step algorithm Verlet-I/r-RESPA [16]. RATTLE algorithm [17] was used to constrain bonds involving hydrogen atoms allowing for 2 fs time steps. Long-range electrostatic forces were updated every two time steps. MD production runs were carried out for 100 ns. To study the effect of the double mutant (R32D, D307R) the last structure from the wild-type simulation was used to generate such mutations, and the simulation was extended for 37 ns. All calculations were performed using the NAMD2.9 [18] software. Important to note is that, very recently, and after the results of the present work were obtained, a low resolution (5.6 Å) cryo-electron microscopy (cryo-EM) structure of the

murine Kir6.2 channel was solved (PDB ID: 5wua), providing the opportunity to check the quality of the homology model used herein. For that purpose the Cα RMSD between the homology model and the cryo-EM structure was computed for the tetramer, for each monomer, and for each monomer split into transmembrane (TMD) and cytoplasmic domains (CTD). The tetramer RMSD accounts for 3.1 Å, indicating a structural similarity within experimental error. Furthermore, considering each monomer separately, an average RMSD of 2.7 Å is obtained, which is decoupled in RMSD values of 1.7 Å and 2.8 Å for the TMD and CTD, respectively. Superimposed structures are shown in Supplementary Fig. S-1A. As an additional confirmation of the homology model quality, the Cα RMSD with respect to the cryo-EM structure was also calculated for the initial structure of the double mutant simulations, which corresponds to the conformation obtained after 100 ns of MD simulations of the wild type channel. In this case, the RMSD for the tetramer is 3.1 Å, the average monomeric RMSD is 2.8 Å, and the RMSD for the monomeric TMDs and CTDs are 1.4 Å and 2.9 Å, respectively. Superimposed structures are shown in Supplementary Fig. S-1B. These results confirm the good quality of the homology model used to initialize the MD simulations presented in the present work.

3. Results

3.1. The sequence of the Kir6.2 N-terminal domain is an additional determinant for the ICCR function

Among ICCRs, the Kir6.2 regulation by the fused GPCR can be either a ligand-induced opening or closing, depending on the fused GPCR. Thus, for example, the human M2 muscarinic receptor opens the ion channel upon acetylcholine (ACh) binding, while $D2_L$ (D2) dopaminergic receptor closes it in the presence of dopamine. In a previous study [3], we demonstrated that the length of the receptor C-termini controls the sign and the amplitude of the channel regulation. In the muscarinic ICCR, the receptor C-ter was shortened by 9 residues in order to mimic the D2 C-ter length, resulting in an inversion of the channel regulation leading to an inhibition of the channel by ACh (Fig. 1A). By extending the D2 C-ter with various sequences of 9 residue-length, the regulation was also inverted (activation by dopamine), demonstrating that the length of the M2 and D2 C-termini finely tunes the Kir6.2 regulation independently of the sequence. The nomenclature used for ICCRs is M2=K to indicate the fusion of the muscarinic M2 receptor to Kir6.2, and addition of a number refers to the size of deletions; for instance -9-25 is a deletion of 9 residues at the receptor C-ter and 25 residues at the Kir6.2 N-ter. Deletion of the first 25 residues was previously identified as optimal for the functional coupling between the fused GPCRs and Kir6.2 [1].

In the present study, we investigate a deletion of identical size (9 residues) in the channel N-terminal domain instead of the receptor C-ter, creating the construct M2=K0-34 (Fig. 1A), which is isometric to M2=K-9-25. However, in M2=K0-34, the regulation of Kir6.2 by M2 is not inverted by the 9-residue deletion and instead, it is abolished as illustrated in Fig. 1B&C. This result indicates that deletion in the channel N-terminal domain affects the ICCR differently than a similar deletion in the receptor C-ter, suggesting the presence of residues in the Kir6.2 N-terminal domain that are critical for the function of ICCR.

To determine the functional impact of the length of the Kir6.2 N-terminal domain, we incrementally deleted it from the 20^{th} to the 34^{th} residue. Fig. 2A illustrates that truncation of the first 20 to 29 residues of Kir6.2 leads to ACh-activated ICCRs with an optimum when 25 residues are deleted (M2=K0-25). After a pivot at position -30 (no regulation), further deletions lead to ACh-inhibited ICCRs until the deletion reaches 34 residues (M2=K0-34) when it shows again an absence of regulation.

When the same approach of incremental deletions was previously used between M2=K0-25 and M2=K-9-25, a linear correlation between the length of the M2 C-ter and the regulation of the channel was observed [3]. In Fig. 2B, these previous results (in blue) are superimposed with

those of Fig. 2A (in red), revealing that, from M2=K0-25, deletions of up to 5 residues in the M2 C-ter or the Kir6.2 N-ter induce similar regulation of the channel. In contrast, further deletions show a discrepancy in the amplitude of ACh-induced inhibition; the inhibition being lower for Kir6.2 N-ter deletions and totally abolished for M2=K0-34.
These results indicate that the composition of the Kir6.2 N-ter sequence is an additional parameter to be considered in the receptor-mediated regulation of Kir6.2.

3.2. Arg27 and Arg32 are sufficient to restore regulation of Kir6.2 by M2

To identify the Kir6.2 residues critical for the ICCR function, we analyzed the sequence alignment of M2=K-9-25 and M2=K0-34 in the only domain that differs between both constructs, the linking domain over a portion of 9 residues. Fig. 3A shows the presence of a cluster of 5 arginines in the Kir6.2 N-ter that is absent in the non-regulated ICCR M2=K0-34. Due to this high density of arginines in the functional ICCR, we suspected that these basic residues had a role in the regulation of ICCRs.
To validate this hypothesis, we used an approach of functional mapping by introducing arginines one by one or two by two in the non-regulated ICCR, in order to restore the function if some arginines are critical. Unexpectedly, introducing arginines R27 (Y459R) or R32 (A464R) alone into M2=K0-34 is sufficient to restore the ACh-evoked inhibition as illustrated in Fig. 3A&B. In contrast, introducing R29 (N461R) or R31 (G463R) does not restore inhibition. The double mutants Y459R/N461R and G463R/A464R were designed in parallel as it was not initially expected that a single arginine could restore the ICCR function. As both double mutants contain either R27 or R32, they also restore the inhibition of Kir6.2 by M2, confirming the role of these arginines in the regulation of the ICCR.

3.3. Arg32 is essential for ICCR function

Reciprocity was tested by mutating the arginines in M2=K-9-25. R27 and R32 were replaced by their matching residues in the M2 sequence (R27Y and R32A, respectively). R29 and R31, that were not sufficient to restore the function, were mutated in tandem (R29N,R31G) as they are not supposed to affect ICCR function. It is found that the mutant R32A is no longer regulated by M2 (Fig. 4), confirming the critical role of this arginine for the function of the ICCR. However, substituting R27 does not abolish channel regulation by M2, indicating that while this arginine was sufficient to restore channel regulation, it is not necessary to maintain it. The absence of effect in the case of the double mutant R29N-R31G confirms the non-essential role of these two arginines.

3.4. Interaction of R32 with C-terminal acidic residues in MD simulations

Residues equivalent to Kir6.2 R34 are highly conserved in the Kir channel family, and they clearly interact in the crystallographic structures [19-23] with a highly conserved glutamate residue in the C-terminal domain. This residue corresponds to glutamate E308 in Kir6.2. However, these structures do not provide information about the position of Kir6.2 R32 because the N-terminal domain is either truncated or the side chain of R32 is unresolved. The positive charges carried by arginines could interact either with the highly negatively-charged PI(4,5)P2 (PIP_2), essential to stabilize Kir channels open state, or with negatively charged acidic residues. To discriminate between these two possibilities, we built a homology model of Kir6.2 based on the crystallographic structure of Kir2.2 [20] with extended N-ter in unstructured form and random orientation. An MD simulation was performed in a time frame of 100 ns during which the N-terminal domain reoriented toward the C-terminal domain as shown in Fig. 5A&B and Supplementary Fig. S-2A. This reorientation of the Kir6.2 N-ter away from the lipid bilayer reinforces the hypothesis that R32 interacts with acidic residues. Analysis of the potential interacting residues revealed that in 52% of the simulated time (Supplementary Fig. S-2B), R32

interacts with aspartate 307 (D307) which is in close proximity to the highly conserved E308 (Fig. 5C).

3.5. Involvement of Kir6.2 C-terminal acidic residues in ICCR function

To test the results of the MD simulations, we mutated the acidic residues potentially interacting with the N-terminal arginines, and characterized their effect on the channel regulation by M2. According to the cluster analysis presented in Supplementary Fig. S-2B, we mutated the acidic residues D307 and E321 as they potentially interact with R32 and R27, respectively. Glutamate E308 was also mutated as a positive control since it is critical for ion channel function [24] and it is predicted to interact with the highly conserved R34, according to the crystallographic structures of Kir channels, and MD simulation results presented herein (Supplementary Fig. S-2B). The acidic residues were mutated to arginines to invert their charge and in order to create electrostatic repulsion with putative interacting arginines.
As expected, a drastic loss of channel regulation of mutant E308R was found as illustrated in Fig. 6A&B. However, while the same loss of channel regulation is found in mutant D307R, mutation E321R does not affect ICCR function. These results indicate that aspartate D307 is involved in ICCR regulation and support a model where D307 interacts with arginine R32.

3.6. The interaction of R32:D323 in the K_{ATP} structure is not involved in the ICCR regulation

Two cryo-electron microscopy structures of the SUR1:Kir6.2 K_{ATP} channels were released at the end of January 2017 with the overall resolution of 5.1 Å [25] (pdb code 5twv) and 5.6Å [26] (pdb code 5wua). The first residue resolved in both structures is R32 however the resolution at this position is not high enough to clearly identify the density of the full length side chain. In the structure solved by Li *et al.* (5wua), coordinates are not available beyond the Cβ and this atom points toward D307 (Supplementary Fig. S3A). In the structure solved by Martin *et al.* (5twv), the side chain of R32 has been modelled and interacts with the side chain of D323 (Supplementary Fig. S3B). In order to determine whether D323 is functionally interacting with R32 in ICCR, we created the mutant D323R and functionally characterized it. The mutant M2=K(D323R)-9-25 is still inhibited by ACh (Fig. 6) indicating that this aspartate residue is not essential for the ion channel regulation by the GPCR.

4. Discussion

In ICCRs, the C-terminus of the receptor is connected to the N-terminus of the Kir6.2 channel creating a linker domain critical for the functional coupling between the two proteins. We previously demonstrated with different receptors that the length of this domain govern the regulation of the channel by the fused receptor. In this study, we found that the length of the receptor C-ter or the channel N-ter is not the only parameters controlling Kir6.2 regulation, but the composition of the Kir6.2 N-terminal sequence in the region Y26-R34 is also essential for ICCR function. A functional mapping approach using isometric constructs (to avoid interference of the length effect) and incorporation of single arginines in the non-regulated construct (M2=K0-34), identified arginines R27 or R32 as sufficient to restore ICCR function. The restoration of ICCR regulation by single arginines suggests a specific role of these arginines within the cluster. Notably, a cluster of positive charges is also present in the same region of all other human Kir channels (Supplementary Fig. S-4). However, except for R34 (Kir6.2), which is highly conserved, the number and the position of the basic residues in Kir channel N-ter are erratic even between isoforms which suggests a variability in their role or in their interaction among the Kir channel family.

The reciprocal approach consisting of substituting arginines in the functional ICCR (M2=K-9-25) revealed that mutating only R32 is sufficient to abolish the regulation, while substituting R27 maintained the ICCR function. This result indicates that R32 is sufficient and essential to restore the function. The ability of R27, the least conserved arginine within the cluster, to restore the function in the absence of R32, suggests that compensation mechanisms occurred in the mutant M2(Y459R)=K0-34 (R27 incorporation). Rearrangement of critical interactions due to removal of a large hydrophobic residue and/or the generation of three concomitant positive charges with the adjacent histidine H458 and lysine K460 might occur (Fig. 3A).

We further explored the role of R32. In Kir channels, the electrostatic potential map reveals a large area of negative surfaces in the extracellular and intracellular domains, and only restricted positive areas in the cytoplasmic domains below the inner leaflet of the lipid bilayer [27]. As the activity of all Kir channels requires the presence of the phospholipid PIP_2, the first obvious hypothesis for the role of R32 is an interaction with PIP_2 molecules. However, while structure-function studies [28,29] and crystallographic structures of Kir channels [20-23] identified several N-terminal basic residues interacting with PIP_2 molecules or with ATP in Kir6.2 [30-32], none of these studies identified R32 or homologous residues as potential interacting partners with PIP_2. Strikingly, a second binding site of negatively charged phospholipids has been discovered in Kir2 channels [23,33] opening the possibility of interactions between the N-terminal basic residues and these lipid molecules that have not been characterized yet. However, multiscale simulations performed to identify PIP_2 binding sites [34], and our own simulations employed to identify molecular interactions of R32 indicate that this arginine is probably not interacting with phospholipids.

A pull-down assay with radiolabeled Kir6.2 C-terminal domain [170-391] [35] demonstrated that residues within the sequence [31-38] are essential for the interaction with the C-terminal domain, supporting a possible role of Kir6.2 R32 in the interaction with the C-terminal domain in addition to R34 and K38.

In an attempt to find any interacting acidic residues in the highly negatively charged surface of the cytoplasmic domain, we created a model of Kir6.2 based on the crystallographic structure of Kir2.2 (PDB code: 3spi) and extended the N-terminal domain of Kir6.2 to include residues from A22 to Q30. Molecular dynamic simulations of such model revealed that R32 interact with D307 (52% of the 100ns simulated time), and the charge inversion mutation (D307R) abolished the regulation of the ICCR. This result clearly identified D307 as an essential residue for the ICCR function. As expected, the same result was obtained for E308, but not for E321, indicating that the latter is not involved in channel regulation by the M2 receptor. As for R32, D307 was not previously identified as a critical residue for Kir6.2 activity, the mutant D307G showing similar ATP sensitivity and basal current to wild-type [24]. However, the mutation E308A confirmed the critical role of this residue as no current was observed for this mutant.

Since the acquisition of these results, two cryo-electron microscopy structures of Kir6.2-based K_{ATP} channels were published (January 2017). The residue R32 is present in both structures but only the structure of Martin *et al.* (5twv) shows a modelled full length side chain of R32 interacting with the aspartate D323. The functional characterization of the mutant D323R within ICCR indicates that D323 is not involved in the regulation of the ion channel while R32 and D307 are, as discussed above. Noteworthy, in the structure of Li *et al.* (5wua), the resolved Cβ of the R32 side chain points toward D307, in the opposite direction of D323.

As R32 is conserved in most Kir channels, we extended this structural analysis to all known structures of Kir channels including structures without transmembrane domains and containing N-ter and C-ter cytoplasmic domains. The results of this analysis are summarized in the table 1 and show a heterogeneity of interaction between Kir6.2 R32-equivalent residues and acidic residues in the C-ter domain, when side-chains have densities. The observed interacting acidic residues in Kir2.2 and Kir3.2 are equivalent to Kir6.2 D280, and to E282 in Kir3.1. Despite the fact that the equivalent residue of R32 is an isoleucine (I55) and not an arginine in Kir3.2, it is

interesting to note that the side chain of I55 is interacting with or close to the equivalent position of Kir6.2 D307. Moreover, ethanol molecules, activator of Kir3 channels, are found interacting at the interface between I55 (R32-equivalent) and residues in the C-ter domain suggesting a role of this region in the regulation of the channel gating.

In physiological conditions, the interaction of R32 could be dynamic with several proximal acidic residues, but among the tested acidic residues (D307,E321 and D323) only D307 clearly demonstrated a role in the allosteric regulation of the channel in ICCR. This could be explain by the position of D307 which is directly connected to the G loop gate by a β strand. Thus, actuation of D307 would propagate to the G loop gate via the β strand resulting in a change of the channel gating.

Consequently, in the design of new ICCRs, the interaction of R32 and D307 must stay intact to propagate the conformational changes of GPCR to the Kir6.2 gates. This interaction could be altered by the proximity of the highly charged cytoplasmic domains of GPCR or G proteins. As an example, the structure of Kir3.2 with Gβγ subunits (4kfm) [22] shows the strong electrostatic interaction at the interface of the ion channel and the Gβ subunit in the LM loop proximal to the channel N-ter I55 (Kir6.2 R32). The interaction of GPCRs, G proteins and β-arrestins with R32 and D307 will be used as a new criteria to identify functional ICCR in molecular models.

5. Conclusions

Light has been shed on the critical role for the ICCR function of a single arginine (R32) among a cluster of 5 arginines in the N-ter of Kir6.2. This result indicates R32 plays a specific function in the allosteric regulation of the ion channel by the fused M2 receptor. Molecular models and mutagenesis studies suggest that the negatively charged D307 would interact with R32, which would functionally connect the Kir6.2 N-ter and C-ter for the gating regulation. This finding suggests also an alternative interaction of the R32 side chain to the one proposed in current structures of K_{ATP} channels.
In the ongoing development of ICCR technology, these results provide new evidence on the molecular determinants required for ICCR function. Several applications are envisioned for this technology such as primary screening of GPCR ligands independently of downstream pathways, tuning cell response of synthetic organisms or designing biosensors for integration in electronic systems.

Acknowledgements

We are grateful to S. Seino (Kobe University, Japan) for mouse Kir6.2 and D. Logothetis (Northeastern University, MA, USA) for M2. CD and LD acknowledges use of Hartree Centre resources in this work and the ARCHER UK National Supercomputing Service (http://www.archer.ac.uk).
This work was supported in part by grants from the Agence Nationale de la Recherche (ICCR project, grant ANR-09-PIRI-0010), from the National Institutes of Health (Grant N°EB007047) and by studentships to M.P. and L.L. from the Commissariat à l'énergie atomique et aux énergies alternatives. The group is a member of the French National Laboratory of Excellence “Ion Channel Science and Therapeutics” (LabEX ICST) funded by a network grant from ANR (ANR-11-LABX-0015-01). L. D. is a SNI (Sistema Nacional de Investigadores; ANII, Uruguay) researcher. The content is solely the responsibility of the authors and does not necessarily represent the official views of the National Institutes of Health.

References

[1] Moreau CJ, Dupuis JP, Revilloud J, Arumugam K, Vivaudou M (2008) Coupling ion channels to receptors for biomolecule sensing. *Nat Nanotechnol* **3**: 620-625

[2] Keramidas A, Lynch JW (2013) An outline of desensitization in pentameric ligand-gated ion channel receptors. *Cell Mol Life Sci* **70**: 1241-1253

[3] Moreau CJ, Revilloud J, Caro LN, Dupuis JP, Trouchet A, Estrada-Mondragón A, Niescierowicz K, Sapay N, Crouzy S, Vivaudou M (2017) Tuning the allosteric regulation of artificial muscarinic and dopaminergic ligand-gated potassium channels by protein engineering of G protein-coupled receptors. *Sci Rep* **7**: 41154

[4] Moreau CJ, Niescierowicz K, Caro LN, Revilloud J, Vivaudou M (2015) Ion channel reporter for monitoring the activity of engineered GPCRs. *Methods Enzymol* **556**: 425-454

[5] Moreau C, Gally F, Jacquet-Bouix H, Vivaudou M (2005) The size of a single residue of the sulfonylurea receptor dictates the effectiveness of K ATP channel openers. *Mol Pharmacol* **67**: 1026-1033

[6] Dupuis JP, Revilloud J, Moreau CJ, Vivaudou M (2008) Three C-terminal residues from the sulphonylurea receptor contribute to the functional coupling between the K_{ATP} channel subunits SUR2A and Kir6.2. *J Physiol* **586**: 3075-3085

[7] Shen MY, Sali A (2006) Statistical potential for assessment and prediction of protein structures. *Protein Sci* **15**: 2507-2524

[8] Klauda JB, Venable RM, Freites JA, O'Connor JW, Tobias DJ, Mondragon-Ramirez C, Vorobyov I, MacKerell AD, Pastor RW (2010) Update of the CHARMM all-atom additive force field for lipids: validation on six lipid types. *J Phys Chem B* **114**: 7830-7843

[9] Jorgensen WL, Chandrasekhar J, Madura JD, Impey RW, Klein ML (1983) Comparison of simple potential functions for simulating liquid water. *J Chem Phys* **79**: 926-935

[10] Beglov D, Roux B (1994) Finite Representation of an Infinite Bulk System - Solvent Boundary Potential for Computer-Simulations. *J Chem Phys* **100**: 9050-9063

[11] Luo Y, Roux B (2010) Simulation of Osmotic Pressure in Concentrated Aqueous Salt Solutions. *J Phys Chem Lett* **1**: 183-189

[12] Lupyan D, Mezei M, Logothetis DE, Osman R (2010) A molecular dynamics investigation of lipid bilayer perturbation by PIP2. *Biophys J* **98**: 240-247

[13] Feller SE, Zhang YH, Pastor RW, Brooks BR (1995) Constant-Pressure Molecular-Dynamics Simulation - the Langevin Piston Method. *J Chem Phys* **103**: 4613-4621

[14] Izaguirre JA, Catarello DP, Wozniak JM, Skeel RD (2001) Langevin stabilization of molecular dynamics. *J Chem Phys* **114**: 2090-2098

[15] Essmann U, Perera L, Berkowitz ML, Darden T, Lee H, Pedersen LG (1995) Smooth Particle Mesh Ewald Method. *J Chem Phys* **103**: 8577-8593

[16] Tuckerman M, Berne BJ, Martyna GJ (1993) Reversible Multiple Time-Scale Molecular-Dynamics - Reply. *J Chem Phys* **99**: 2278-2279

[17] Andersen HC (1983) Rattle - a Velocity Version of the Shake Algorithm for Molecular-Dynamics Calculations. *j comput phys* **52**: 24-34

[18] Phillips JC, Braun R, Wang W, Gumbart J, Tajkhorshid E, Villa E, Chipot C, Skeel RD, Kalé L, Schulten K (2005) Scalable molecular dynamics with NAMD. *J Comput Chem* **26**: 1781-1802

[19] Tao X, Avalos JL, Chen J, MacKinnon R (2009) Crystal structure of the eukaryotic strong inward-rectifier K^+ channel Kir2.2 at 3.1 A resolution. *Science* **326**: 1668-1674

[20] Hansen SB, Tao X, Mackinnon R (2011) Structural basis of PIP2 activation of the classical inward rectifier K^+ channel Kir2.2. *Nature* **477**: 495-498

[21] Whorton MR, Mackinnon R (2011) Crystal structure of the mammalian GIRK2 K^+ channel and gating regulation by G proteins, PIP2, and sodium. *Cell* **147**: 199-208

[22] Whorton MR, Mackinnon R (2013) X-ray structure of the mammalian GIRK2-ßγ G-protein complex. *Nature* **498**: 190-197
[23] Lee SJ, Ren F, Zangerl-Plessl EM, Heyman S, Stary-Weinzinger A, Yuan P, Nichols CG (2016) Structural basis of control of inward rectifier Kir2 channel gating by bulk anionic phospholipids. *J Gen Physiol* **148**: 227-237
[24] Cukras CA, Jeliazkova I, Nichols CG (2002) Structural and functional determinants of conserved lipid interaction domains of inward rectifying Kir6.2 channels. *J Gen Physiol* **119**: 581-591
[25] Martin GM, Yoshioka C, Rex EA, Fay JF, Xie Q, Whorton MR, Chen JZ, Shyng SL (2017) Cryo-EM structure of the ATP-sensitive potassium channel illuminates mechanisms of assembly and gating. *eLife* **6**: pii: e24149
[26] Li N, Wu JX, Ding D, Cheng J, Gao N, Chen L (2017) Structure of a Pancreatic ATP-Sensitive Potassium Channel. *Cell* **168**: 101-110
[27] Fürst O, Mondou B, D'Avanzo N (2014) Phosphoinositide regulation of inward rectifier potassium (Kir) channels. *Front Physiol* **4**: 404
[28] Cukras CA, Jeliazkova I, Nichols CG (2002) The role of NH2-terminal positive charges in the activity of inward rectifier K_{ATP} channels. *J Gen Physiol* **120**: 437-446
[29] Schulze D, Krauter T, Fritzenschaft H, Soom M, Baukrowitz T (2003) Phosphatidylinositol 4,5-bisphosphate (PIP2) modulation of ATP and pH sensitivity in Kir channels. A tale of an active and a silent PIP2 site in the N terminus. *J Biol Chem* **278**: 10500-10505
[30] Tucker SJ, Gribble FM, Proks P, Trapp S, Ryder TJ, Haug T, Reimann F, Ashcroft FM (1998) Molecular determinants of K_{ATP} channel inhibition by ATP. *EMBO J* **17**: 3290-3296
[31] John SA, Weiss JN, Ribalet B (2005) ATP sensitivity of ATP-sensitive K^+ channels: role of the gamma phosphate group of ATP and the R50 residue of mouse Kir6.2. *J Physiol* **568**: 931-940
[32] Ribalet B, John SA, Weiss JN (2003) Molecular basis for Kir6.2 channel inhibition by adenine nucleotides. *Biophys J* **84**: 266-276
[33] Lee SJ, Wang S, Borschel W, Heyman S, Gyore J, Nichols CG (2013) Secondary anionic phospholipid binding site and gating mechanism in Kir2.1 inward rectifier channels. *Nat Commun* **4**: 2786
[34] Stansfeld PJ, Hopkinson R, Ashcroft FM, Sansom MS (2009) PIP(2)-binding site in Kir channels: definition by multiscale biomolecular simulations. *Biochemistry* **48**: 10926-10933
[35] Tucker SJ, Ashcroft FM (1999) Mapping of the physical interaction between the intracellular domains of an inwardly rectifying potassium channel, Kir6.2. *J Biol Chem* **274**: 33393-33397
[36] Pegan S, Arrabit C, Zhou W, Kwiatkowski W, Collins A, Slesinger PA, Choe S (2005) Cytoplasmic domain structures of Kir2.1 and Kir3.1 show sites for modulating gating and rectification. *Nat Neurosci* **8**: 279-287
[37] Pegan S, Arrabit C, Slesinger PA, Choe S (2006) Andersen's syndrome mutation effects on the structure and assembly of the cytoplasmic domains of Kir2.1. *Biochemistry* **45**: 8599-8606
[38] Nishida M, MacKinnon R (2002) Structural basis of inward rectification: cytoplasmic pore of the G protein-gated inward rectifier GIRK1 at 1.8 A resolution. *Cell* **111**: 957-965
[39] Nishida M, Cadene M, Chait BT, MacKinnon R (2007) Crystal structure of a Kir3.1-prokaryotic Kir channel chimera. *EMBO J* **26**: 4005-4015
[40] Xu Y, Shin HG, Szép S, Lu Z (2009) Physical determinants of strong voltage sensitivity of K^+ channel block. *Nat Struct Mol Biol* **16**: 1252-1258
[41] Inanobe A, Nakagawa A, Kurachi Y (2011) Interactions of cations with the cytoplasmic pores of inward rectifier K^+ channels in the closed state. *J Biol Chem* **286**: 41801-41811

[42] Inanobe A, Matsuura T, Nakagawa A, Kurachi Y (2011) Inverse agonist-like action of cadmium on G-protein-gated inward-rectifier K^+ channels. *Biochem Biophys Res Commun* **407**: 366-371

[43] Inanobe A, Nakagawa A, Matsuura T, Kurachi Y (2010) A structural determinant for the control of PIP2 sensitivity in G protein-gated inward rectifier K^+ channels. *J Biol Chem* **285**: 38517-38523

Figure 1

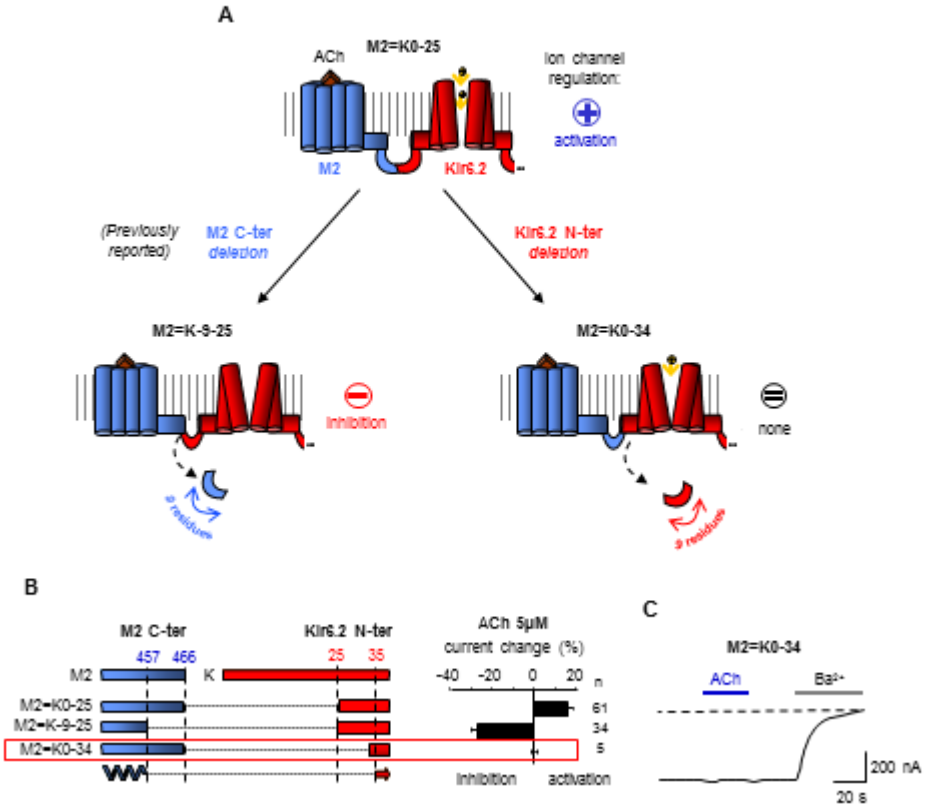

Fig. 1. Ligand-induced regulation of variants of muscarinic M2 Ion Channel-Coupled Receptors (ICCRs). (A) The ICCR M2=K0-25 was previously created by fusing genetically the C-ter of the M2 receptor to the N-ter of the Kir6.2 inward-rectifier potassium channel deleted of its first 25 residues. The fusion protein homotetramerizes to form a complex of 4 Kir6.2 subunits (forming the pore) surrounded by 4 M2 receptors. Only one full-length subunit and the channel of a second subunit are depicted. Binding of acetylcholine (ACh) onto M2 induces an activation of the ion channel. Flow of K^+ ions is inward in our two-electrode voltage-clamp (TEVC) recordings at -50mV in 91 mM K^+ extracellular concentration. A previous study [3] showed that deletion of the last 9 residues of M2 (M2=K-9-25) inverted the channel regulation by ACh. In the present study, we characterize the isometric deletion in the ion channel N-ter (M2=K0-34). (B) Alignment of the indicated constructs with deletions in the M2 C-ter (blue) and the Kir6.2 N-ter. The helix VIII from M2 and the β bridge from Kir6.2 are shown under the alignment. The bar chart displays the percent change ± s.e.m in current induced by ACh 5µM. Positive and negative values indicate activation and inhibition of the channel respectively. Numbers besides bars are the number of tested oocytes (n). The red box around M2=K0-34 indicate the new result obtain compared to the previous ones (M2=K0-25 and M2=K -9-25). (C) Representative TEVC recordings of the indicated constructs. Concentrations of ACh and Ba^{2+} are 5µM and 3mM respectively. Ba^{2+} is a Kir6.2 channel blocker. The dashed line indicates the current after barium block.

Figure 2

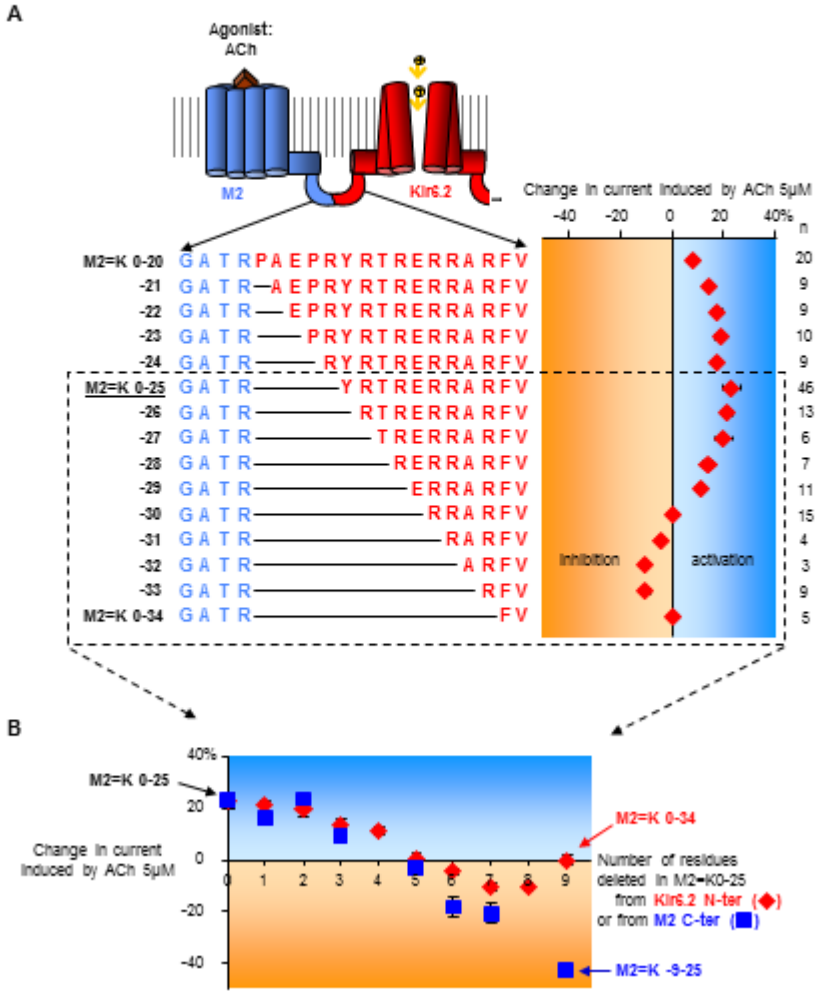

Fig. 2. Kir6.2 channel regulation is not correlated to the length of its N-ter for the largest deletions. (A) Alignment of the linking domain between M2 and Kir6.2 for incremental deletions in the Kir6.2 N-ter. For each construct, the ACh-induced current in percent is plotted at right. The n values represent the number of tested oocytes. (B) The data within the dashed-line box of panel (A) are overlayed onto data obtained previously by truncation of the receptor C-ter [3]. The abscissa axis represents the number of deleted residues from the construct M2=K0-25 either in the M2 C-ter (blue dots) or in the Kir6.2 N-ter (red dots).

Figure 3

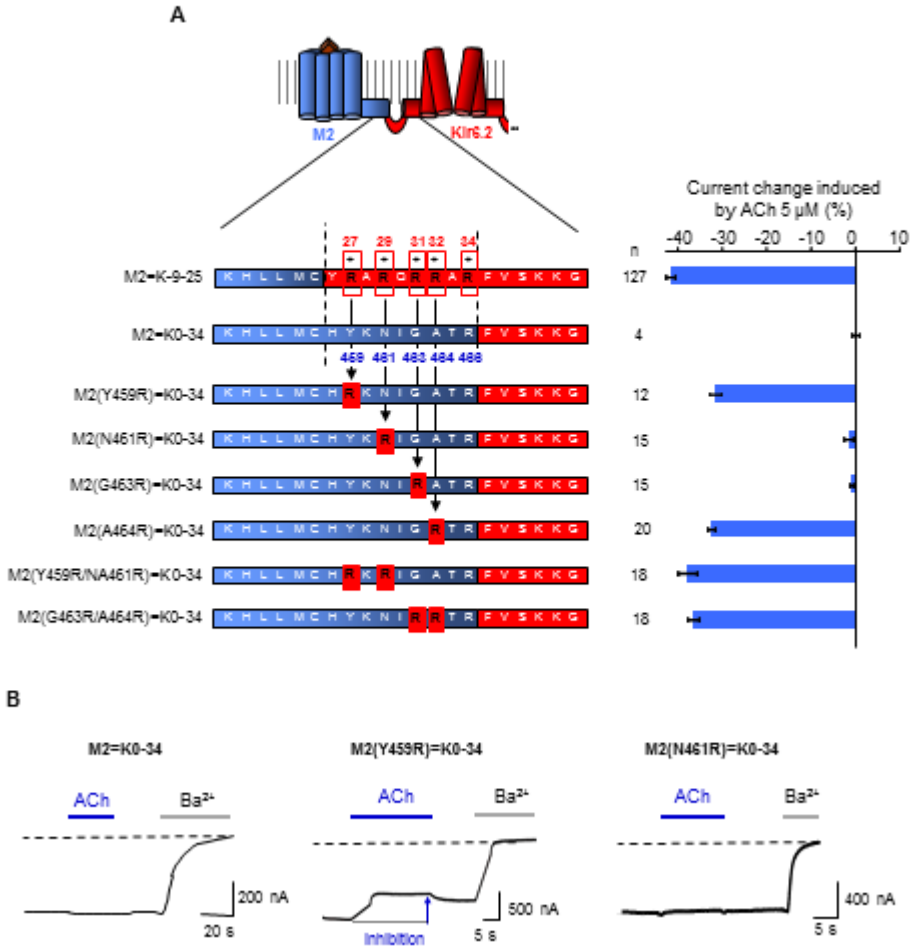

Fig. 3: Role of the cluster of arginine in the N-ter of Kir6.2 in the ICCR function. (A) Alignment of the isometric constructs M2=K-9-25 and M2=K0-34 that are inhibited and unaffected by ACh respectively. A cluster of 5 arginines is present in the N-ter domain of Kir6.2 of the ligand-regulated ICCR (M2=K-9-25). Amino acid numbers refer to the isolated proteins, Kir6.2 (red sequence) and M2 (blue sequence). Mutants of M2=K0-34 by residue-substitution to arginine and their regulation by ACh 5µM represented as mean of the current change ± s.e.m. Number of recordings are indicated beside the bars. (B) TEVC recordings showing the absence of regulation of the wild-type M2=K0-34 and the mutant N461R, and the restoration of the inhibition of the mutant Y459R.

Figure 4

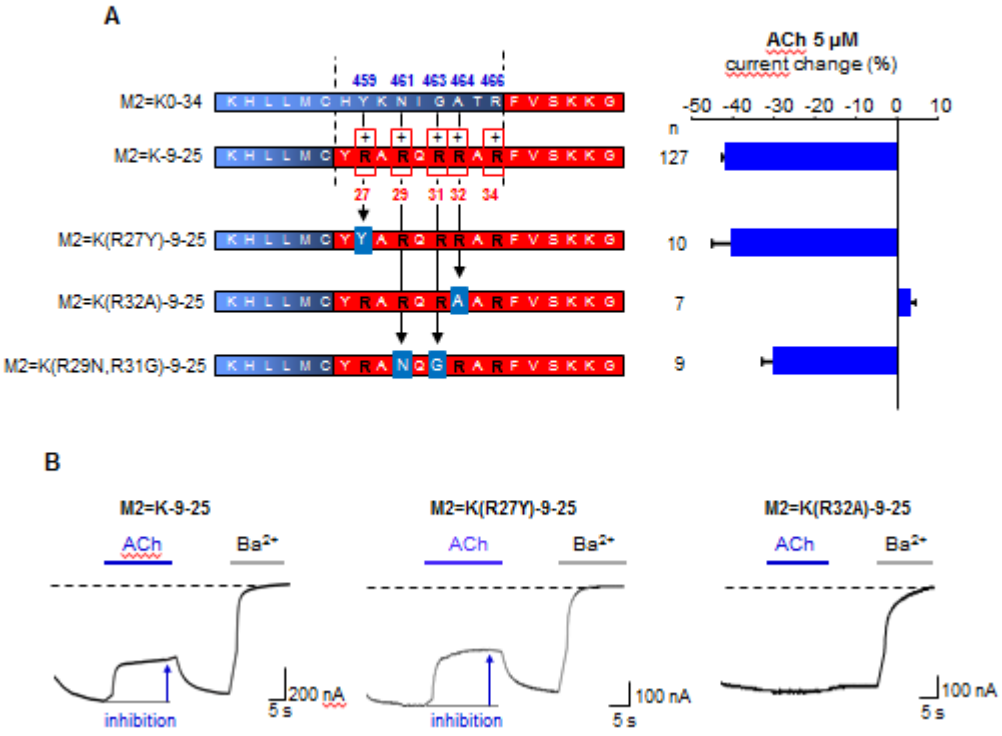

Fig. 4. The essential role of arginine R32 in the allosteric regulation of the ICCR. (A) Alignment of M2=K-9-25 with mutants where arginines are replaced by residues from M2. The bar chart shows the ACh-induced change in current. (B) Representative TEVC recordings showing the loss of ACh-induced inhibition of the mutant R32A.

Figure 5

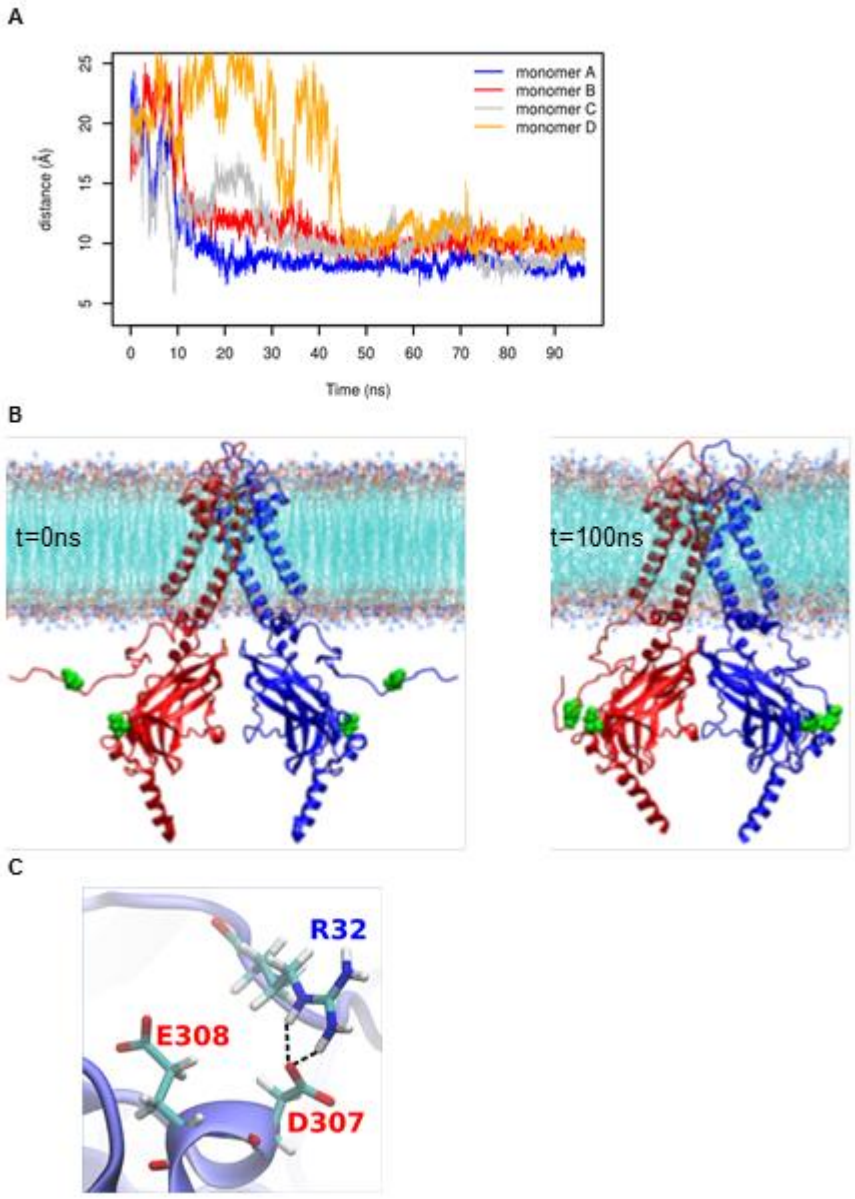

Fig. 5: Interaction between the N-ter segment and the C-ter cytoplasmic domain in Kir6.2 from molecular dynamics simulations. (A) Distance between the Cα of R29 in the Kir6.2 N-ter and the Cα of residue D280 in the cytoplasmic domain for the four monomeric units during 100ns of molecular dynamics simulation. The spontaneous motion of the positive cluster in the N-ter toward the cytoplasmic domain is evidenced. (B) Structure of the channel (only two monomers are shown for clarity) at t=0 ns and t=100 ns, revealing the conformation adopted by the N-ter segments, bound to the cytoplasmic domain. Residues R29 and D280 are indicated in green van der Waals representation. (C) Close-up view of the interaction between R32 and D307 and of the neighbouring highly conserved E308 after the 100 ns simulation. The dotted lines show the hydrogen bonds.

Figure 6

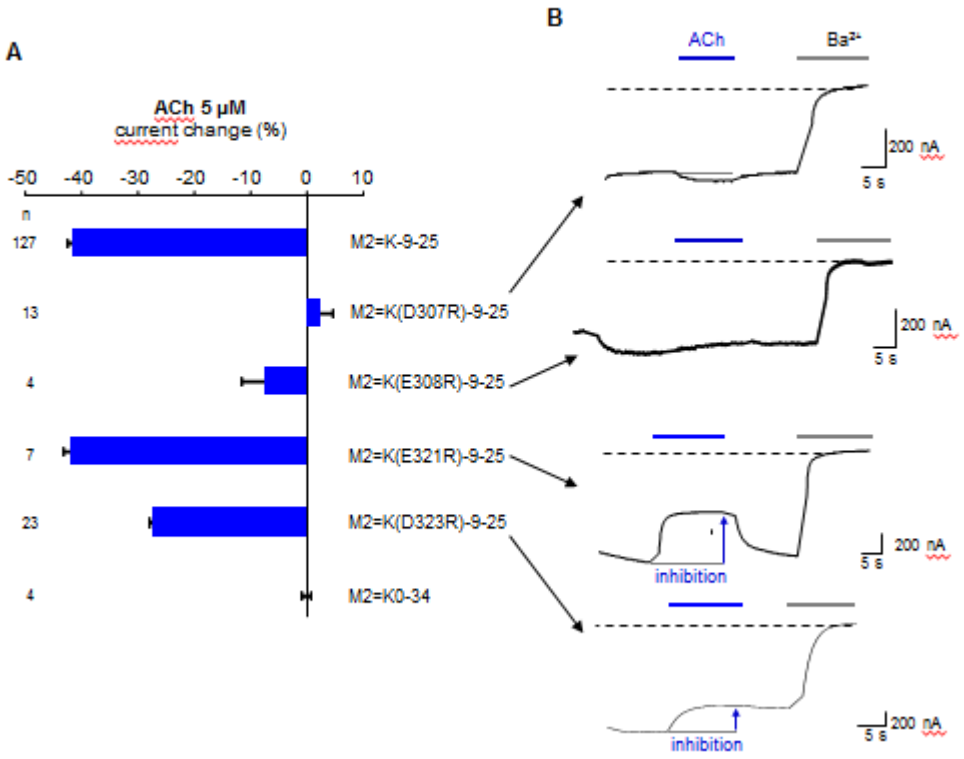

Fig. 6. Role of Kir6.2 C-terminal acidic residues in ICCR function. (A) The bar chart shows the ACh-induced change in current. (B) Representative TEVC recordings of the indicated constructs.

Kir channel	Pdb code	Cytoplasmic domain?	Equivalent residue to Kir6.2 R32	Interacting residue with Eq. R32	Reference
KATP (SUR1:Kir6.2)	5twv		R32 (Modelled side chain)	**D323**	[25]
	5wua		R32 (No density after Cβ)	? (pointing toward D307)	[26]
Kir2.1	1u4f	Cytoplasmic domain	R44	None	[36]
	2gix	Cytoplasmic domain	Not present in the structure		[37]
Kir2.2	3spc, 3spg, 3sph, 5kuk, 5kum		R42	D292 (eq **D280**)	[20] [23]
	3spi		R42 (No density after Cβ)	? (Cβ pointing toward S319 (Eq. D307) and opposite to D292 (Eq. D280)	[20]
	3spj, 3jyc		Not present in the structure		[20] [19]
Kir3.1	1np9, 1u4e	Cytoplasmic domain	R43	E294(Eq. **E282**) E318 (Eq. ***A306***)	[38] [36]
	2qks	chimera	R5 (Subunits with and without side chain)	Q239 (T224) E265 (***A306***)	[39]
	3k6n	Cytoplasmic domain	Not present in the structure		[40]
Kir3.2	2e4f	Cytoplasmic domain	I55	S330 (Eq. **D307**) I328 (Eq. L305)	To be published
	3ata, 3atb, 3ate	Cytoplasmic domain	I55	E303 (Eq. **D280**) I328 (Eq. L305) T329 (Eq. ***A306***)	[41]
	3auw (pbdb 1 and 2)	Cytoplasmic domain	I55	E303 (Eq. **D280**) I328 (Eq. L305) T329 (Eq. ***A306***) **Ethanol**	[42]
	3agw	Cytoplasmic domain	I55	E303 (Eq. **D280**) I328 (Eq. L305) **Ethanol**	[43]
	3at8, 3at9, 3atd	Cytoplasmic domain	I55	E303 (Eq. **D280**) I328 (Eq. L305)	[41]

	3syp		I55	Y349 (Eq. Y326)	[21]
	3syq		I55 (Half subunits with side chain density)	None	[21]
	3sya, 3syc, 3syo, 4kfm		I55 (No side chain density)		[21] [22]
	3atf, 3vsq	Cytoplasmic domain	Not present in the structure		[41] To be published

Table1. Structural analysis of the interaction of R32 and R32-equivalent residues in known structures of Kir channels. Structures without transmembrane domains are indicated as "cytoplasmic domain". In red are indicated D307 or A306 (close to D307) and in blue other acidic residues. Eq. means equivalent residue in Kir6.2. Interacting residues interact with Eq. R32 side chain 5 Å around Cζ.

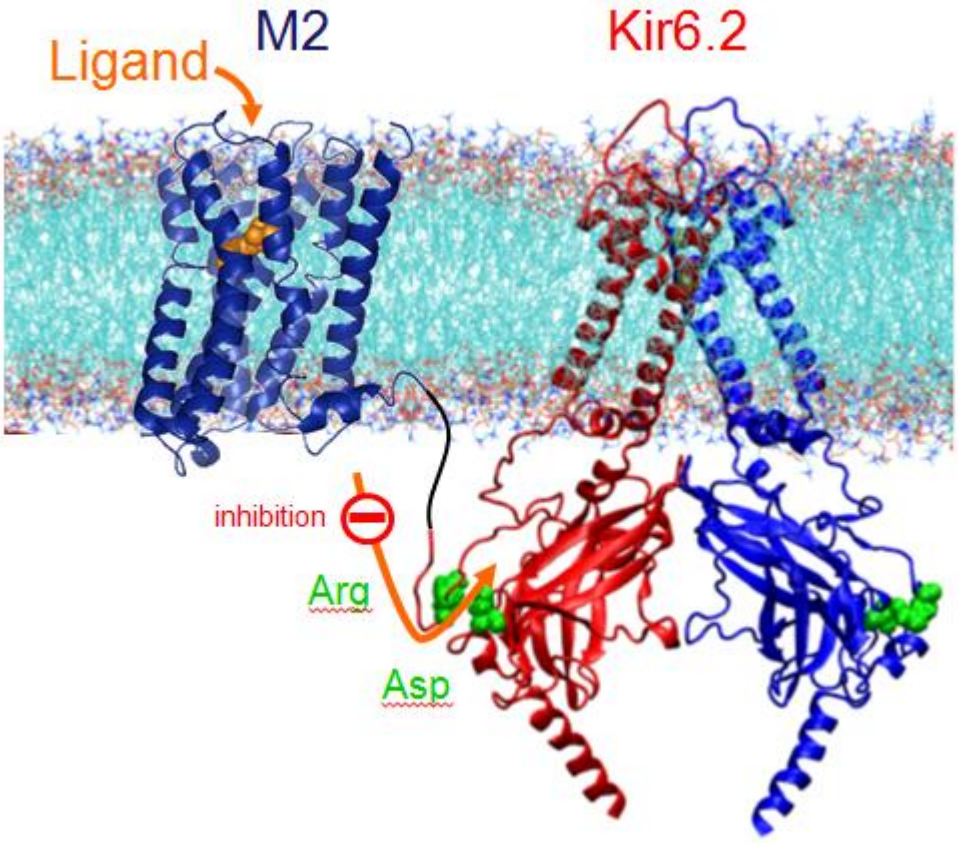

Graphical abstract

Functional Mapping of the N-terminal Arginine Cluster and C-terminal Acidic Residues of Kir6.2 Channel Fused to a G Protein-Coupled Receptor

Maria A. Principalli, Laura Lemel, Anaëlle Rongier, Anne-Claire Godet, Karla Langer, Jean Revilloud, Leonardo Darré, Carmen Domene, Michel Vivaudou and Christophe J. Moreau.

Highlights

- Ion channel-coupled receptors (ICCRs) are artificial ligand-gated ion channels.
- An arginine from the N-ter domain of Kir6.2 is critical for the ICCR function.
- An aspartate from the C-ter domain of Kir6.2 channel is also essential.
- Molecular dynamics simulations suggest a salt bridge between both residues.
- These molecular determinants are required for designing functional ICCRs.